

# BLIND COMPENSATION OF FREQUENCY-SELECTIVE I/Q IMBALANCES IN QUADRATURE RADIO RECEIVERS: CIRCULARITY -BASED APPROACH

Lauri Anttila, Mikko Valkama, and Markku Renfors

Tampere University of Technology  
Institute of Communications Engineering  
P.O. Box 553, FIN-33101 Tampere, Finland

## ABSTRACT

Gain and phase differences between the analog in-phase (I) and quadrature (Q) branches of a quadrature receiver are unavoidable, and seriously degrade its image rejection capabilities. Furthermore, this so-called I/Q imbalance problem is in general a frequency-dependent phenomenon, which is often ignored in many otherwise excellent work. In this paper, we take this frequency-dependency into account and study a class of I/Q imbalance compensators based on widely linear (WL) processing of the received mismatched signal, under the assumption that the ideal baseband signal is proper (or circular). In other words, the complementary autocorrelation function of the ideal baseband signal is assumed to vanish, which is a valid assumption for most practical communications signals. Under I/Q imbalance the observed baseband equivalent signal becomes improper, and I/Q imbalance compensation can be performed by making the observation proper again. We propose a simple blind (non-data aided) WL compensator structure for suppressing the mirror-frequency interference. It shows impressive performance and has many additional desirable features, such as immunity to channel noise and the fading channel.

**Index Terms** — Adaptive filters, circular random signals, I/Q imbalance, mirror-frequency interference, quadrature (I/Q) receivers

## 1. INTRODUCTION

Receivers based on quadrature (or I/Q) downconversion, namely the direct-conversion and the low-IF structure, are gaining more and more interest in both the research community and the industry [1],[2],[4],[5]. They seem to strike a balance between reconfigurability and flexibility on one hand and implementation cost and size on the other. Also, recent research has shown that the well-known problems with the implementation of this type of receivers – namely DC-offsets, receiver nonlinearities, and I/Q imbalance – can be effectively mitigated by careful circuit design (see, e.g., [1],[4]) and/or by using sophisticated digital signal processing (DSP) [3], [5]-[10].

The research on DSP-based I/Q imbalance compensation has been very active in the last decade, covering both blind and data-aided approaches (see, e.g., [5]-[10] and the references therein). However, very few blind techniques are available at

the moment for compensating frequency-dependent imbalances. The WL compensation idea has been utilized recently – in addition to the authors' previous work in [7] and [9] – at least in [6] and [10], both of which assumed OFDM modulation together with known pilot data.

The central theme in this paper is to study DSP-based mitigation of the image or mirror-frequency interference problem caused by I/Q mismatches. More specifically, we propose an adaptive compensation algorithm that uses widely linear filtering of the received baseband signal, utilizing a property of the ideal baseband equivalent signal called *properness* (terminology of [11],[13], or *circularity* in [12]). A random complex signal  $z(t)$  is defined *proper* if its complementary autocorrelation function equals zero:  $c_z(\tau) = E[z(t)z(t-\tau)] = 0 \forall \tau$ , with  $E[\cdot]$  denoting the expectation operator. This assumption is valid for most practical complex alphabets and the resulting waveforms.

The proposed algorithm is capable of operating in any quadrature receiver setting, whether single-channel or multi-channel, and is in fact independent of any specific structure or characteristic of the ideal baseband equivalent signal other than properness. It also takes the possible frequency-dependent nature of the I/Q imbalance into account. The algorithm can be viewed as an extension of the algorithm in [7] to the frequency-dependent imbalance case.

## 2. FREQUENCY-SELECTIVE I/Q IMBALANCES

The modeling of I/Q imbalance is split into two parts: a frequency-independent and a frequency-dependent part. The frequency-independent portion is modeled by an imbalanced complex local oscillator (LO) as [5],[14]

$$s_{\text{LO}}(t) = \cos(\omega_{\text{LO}}t) - jg \sin(\omega_{\text{LO}}t + \phi) \\ = K_1 \exp(-j\omega_{\text{LO}}t) + K_2 \exp(j\omega_{\text{LO}}t) \quad (1)$$

with  $g$  and  $\phi$  denoting the amplitude and phase imbalance parameters (ideally  $g = 1$  and  $\phi = 0$ ), respectively, and  $\omega_{\text{LO}} = 2\pi f_{\text{LO}}$  the angular frequency of the local oscillator. The imbalance coefficients  $K_1$  and  $K_2$  are given by

$$K_1 = \frac{1 + g \exp(-j\phi)}{2} \quad \text{and} \quad K_2 = \frac{1 - g \exp(j\phi)}{2} \quad (2)$$

The above model is widely used in modeling I/Q imbalances that are independent of frequency (see for example [5]-[10],[14]). To extend this model to include also the frequency-dependency of the mismatches, the *generalized imbalance*

This work was supported by Nokia Oyj, Nokia Foundation, the Technology Development Foundation of Finland, the Technology Industries of Finland Centennial Foundation, and the Academy of Finland.

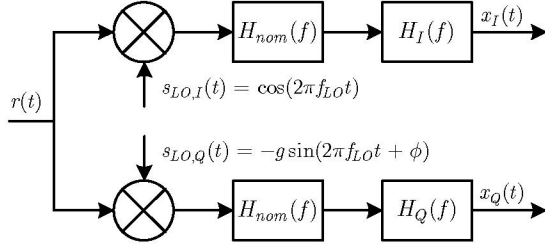


Fig. 1. Generalized I/Q imbalance model for the analog front-end.

*model*, including both the frequency-independent and dependent imbalances, is introduced in Fig. 1 [5]. The model includes the nominal frequency responses of the branches  $H_{nom}(f)$  (due to, e.g., low-pass filters), while  $H_I(f)$  and  $H_Q(f)$  represent the portions in I and Q amplitude and phase responses that differ from the nominal response. With perfect matching  $H_I(f) = H_Q(f) = 1$ . For now, we let  $H_{nom}(f) = 1$  without loss of generality.

We denote the ideal baseband equivalent of the received signal or signal band by  $z(t)$ , with Fourier transform (FT)  $Z(f)$ . In general,  $z(t)$  can contain an arbitrary number of modulated carriers on adjacent IF channels, and all RF disturbances up to the I/Q downconversion stage, including, e.g., the additive noise and the (possibly) fading channel. After some simple manipulations, the imbalanced signal can be expressed, in terms of FT's, as [5]

$$X(f) = G_1(f)Z(f) + G_2(f)Z^*(-f) \quad (3)$$

The frequency responses  $G_1(f)$  and  $G_2(f)$  of the direct and of the conjugated signal contributions are defined in (4) [5].

$$\begin{aligned} G_1(f) &= [H_I(f) + H_Q(f)g \exp(-j\phi)]/2 \\ G_2(f) &= [H_I(f) - H_Q(f)g \exp(j\phi)]/2 \end{aligned} \quad (4)$$

In (3), the term relative to  $Z^*(-f)$  represents the mirror-frequency interference caused by the imbalances. Clearly, if  $H_I(f) = H_Q(f) = 1$ ,  $g = 1$  and  $\phi = 0$ , the conjugate term disappears, and  $X(f) = Z(f)$ . Based on (3), the image attenuation of the whole analog front-end is now defined as

$$A_{FE}(f) = \frac{|G_1(f)|^2}{|G_2(f)|^2} \quad (5)$$

By applying the inverse FT, the signal model of (3) is expressed in time domain as

$$x(t) = g_1(t) * z(t) + g_2(t) * z^*(t) \quad (6)$$

The signal model of the above type is often termed *widely linear* (WL), indicating the linear dependency of  $x(t)$  on both  $z(t)$  and  $z^*(t)$  [11],[12]. Analogously to (3), the conjugate term in (6) is the source of the image interference. From the above discussion, it is now obvious that to suppress the image interference, we need to somehow remove or mitigate this conjugate signal term. This is indeed the goal of this paper, i.e., to study DSP-based mitigation of the conjugate signal term in (3) and (6) (manifesting itself as image interference), based on certain second-order statistical properties of the ideal and mismatched baseband equivalents  $z(t)$  and  $x(t)$ . This was also the

basic working assumption in the previous publications [7] and [9], but in the frequency-independent imbalance case.

### 3. SECOND-ORDER STATISTICS OF I/Q SIGNALS

The ideal baseband equivalent  $z(t) = z_I(t) + jz_Q(t)$  is here assumed to be proper, meaning that its complementary autocorrelation function vanishes [11]-[13]:

$$c_z(\tau) = E[z(t)z(t - \tau)] = 0 \quad \forall \tau \quad (7)$$

Interpreting this in terms of the statistics of  $z_I(t)$  and  $z_Q(t)$ , (7) means that the I and Q signals have identical autocorrelation functions and an odd cross-correlation function [13]. In most practical cases, the cross-correlation function is identically zero. Yet another, useful, interpretation of (7) is that  $z(t)$  and  $z^*(t)$  are *mutually uncorrelated*, because  $E[z(t)z(t - \tau)] = E[z(t)(z^*(t - \tau))^*] = E[z(t)(z^*(t - \tau))] = 0$ . Most practical complex-valued alphabets and their waveforms fulfill the criterion in (7), excluding real-valued modulations such as BPSK. [11]-[13]

It is now straightforward to show that I/Q imbalance makes the observed baseband signal (6) *improper*, its complementary autocorrelation function now being of the form

$$\begin{aligned} c_x(\tau) &= E[x(t)x(t - \tau)] = \dots \\ &= \int_{-\infty}^{\infty} \int_{-\infty}^{\infty} g_1(\lambda_1)g_2(\lambda_2)\gamma_z(\tau + \lambda_2 - \lambda_1)d\lambda_1d\lambda_2 \\ &\quad + \int_{-\infty}^{\infty} \int_{-\infty}^{\infty} g_1(\lambda_3)g_2(\lambda_4)\gamma_z(-\tau + \lambda_4 - \lambda_3)d\lambda_3d\lambda_4 \neq 0 \end{aligned}$$

Here,  $\gamma_z(\tau) = E[z(t)z^*(t - \tau)]$  is the ordinary *autocorrelation function* of  $z(t)$ , and  $g_1(t), g_2(t) \neq 0$ . The I/Q imbalance compensation strategy, to be addressed in the next section, is then to map the observed signal back to the “proper domain” by using adaptive filtering techniques.

### 4. I/Q IMBALANCE COMPENSATION USING ADAPTIVE WIDELY LINEAR FILTERING

Here we develop an adaptive algorithm for mitigating the mirror-frequency interference, utilizing the assumption that the ideal baseband signal is proper. Under this assumption, the compensation of the image interference amounts to making the observed signal proper again. We also discuss some practical aspects of I/Q imbalance compensation in general.

#### 4.1 The Adaptive Algorithm

Considering the WL signal model (6), it is intuitively clear that for removing the conjugate term, a WL compensator structure of the general form in (8) can be used:

$$y(n) = \mathbf{w}_1^T \mathbf{x}(n) + \mathbf{w}_2^T \mathbf{x}^*(n) \quad (8)$$

Here, we have switched to discrete-time notation, and define  $\mathbf{w}_i = [w_i(0) w_i(1) \dots w_i(N-1)]^T$ ,  $i = 1, 2$  as the compensator filters,  $\mathbf{x}(n) = [x(n) x(n-1) \dots x(n-N+1)]^T$  as the input vector to the compensator, while  $N$  is the length of the filters. To remove the conjugate term, it is now enough that the transfer functions of  $\mathbf{w}_1$  and  $\mathbf{w}_2$  satisfy the condition  $W_2(z)/W_1(z) = -G_2(z)/G_1^*(z^*)$ , with  $G_1(z)$  and  $G_2(z)$  denoting the transfer functions of  $g_1(n)$  and  $g_2(n)$ , respectively. Clearly,  $W_1(z)$  is redundant, and we can set  $W_1(z) = 1$ , thus needing only the

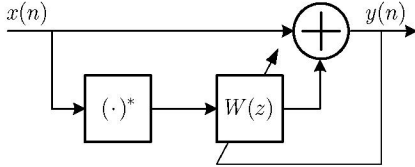


Fig. 2. Proposed WL I/Q imbalance compensator structure.

filter in the conjugate signal path. The final form of the compensator becomes

$$y(n) = x(n) + \mathbf{w}^T \mathbf{x}^*(n) \quad (9)$$

which is also illustrated in the block diagram of Fig. 2.

The optimum solution for the sole filter  $\mathbf{w}$ , in the sense that it mitigates the conjugate term completely, is

$$W_{OPT}(z) = -G_2(z) / G_1^*(z^*) \quad (10)$$

The impulse response of the above optimum solution is, in general, infinitely long. However, assuming that  $H_I(f)$  and  $H_Q(f)$  can be modeled as short FIR filters,  $G_1(z)$  and  $G_2(z)$  will also be short FIR filters. This is especially true for the impulse response of  $G_1(z)$ , which is in practice close to a pure impulse. Therefore,  $W(z)$  can be accurately approximated with a relatively short FIR filter.

The problem then boils down to finding a proper, blind, update rule for the adaptive filter coefficients. The goal is to make the output of the compensator proper, i.e., to have  $E[\mathbf{y}(n)\mathbf{y}(n)] = \mathbf{0}$  at the output. A simple algorithm of the form

$$\begin{cases} \mathbf{y}(n) = \mathbf{x}(n) + \mathbf{w}^T(n) \mathbf{x}^*(n) \\ \mathbf{w}(n+1) = \mathbf{w}(n) - \mathbf{M} \mathbf{y}(n) \mathbf{y}(n) \end{cases} \quad (11)$$

with output vector  $\mathbf{y}(n) = [y(n) \ y(n-1) \ \dots \ y(n-N+1)]^T$  and step-size matrix  $\mathbf{M} = \text{diag}(\mu_1, \mu_2, \dots, \mu_N)$ , will accomplish this, since in the steady state we will indeed have  $E[\mathbf{y}(n)\mathbf{y}(n)] = \mathbf{0}$ . To give the algorithm some further formal justification, it can be interpreted as a “stochastic” Newton zero search in the function  $f(\mathbf{w}) = E[\mathbf{y}(n)\mathbf{y}(n)]$ .

Notice also, that the stability point of the algorithm is not unique, since properness at the output is obtained with two possible filters: the optimum solution in (10), and the *conjugate solution*  $W_C(z) = -G_1(z) / G_2^*(z^*)$  which results in complete suppression of the *desired signal term*. However, by initializing the filter with all zeros, convergence in the direction of the optimum solution is in practice guaranteed, since the origin is in the attraction domain of the optimum solution.

#### 4.2 Practical Aspects

The widely linear compensator structure and the proposed multi-tap compensator in (11) have several advantageous features from the practical point of view. First, the ideal baseband equivalent  $z(t)$  can be here viewed to contain, in addition to the desired signals and the RF image signals, also *all RF disturbances up to the I/Q downconversion stage*, including, e.g., the channel noise, the effects of a fading multipath channel, and also any frequency offsets in the system. Thus, the algorithm has fundamental robustness against the major RF non-idealities.

Another major benefit of the algorithm is its generality: (1) it can be applied to any quadrature receiver structure, whether single-channel or multi-channel and (2) no assumptions on the ideal received signal need be made except its properness.

The algorithm is also relatively simple to implement. It requires  $8N + 1$  or  $10N - 1$  real multiplications (depending on whether the same step-size for all the taps or a different step-size for each tap is used), and  $6N + 1$  real additions per update cycle, with  $N$  denoting the length of the filter. By selecting the step-size a power of two, some further reduction in the number of multiplications is achieved. In other words, the complexity is very similar to that of the basic LMS channel equalizer. Only the number of delay elements is doubled, since both the input and the output need to be stored (see (11)). These figures do not take into account the estimation of the received signal power, which is also necessary in practice in determining the algorithm step-size.

Also, as will be shown in the next section through simulations, the algorithm tends to equalize the signal-to-image power ratio of the processed band. This, combined with the adaptive nature of the algorithm, i.e., its ability to track the time-varying dynamics in the received signal and the time-variations in the imbalance parameters, and the other desirable features stated above, makes the proposed algorithm of great practical interest.

#### 5. PERFORMANCE SIMULATIONS AND NUMERICAL ILLUSTRATIONS

Here the performance of the proposed algorithm is evaluated through simulations in terms of image rejection ratios and symbol-error-rates for 16-QAM signals. We consider a two-carrier receiver, with the two signals sitting at mirror intermediate frequencies. The imbalanced local oscillator (LO) mismatch levels are 3% in amplitude and 3° in phase, and the branch filter non-idealities are of the form  $H_I(z) = 0.98 + 0.03z^{-1}$  and  $H_Q(z) = 1.0 - 0.005z^{-1}$ . The front-end IRR was defined in (5), and in the given example case it has roughly 10 dB dynamics, the minimum IRR being ~25 dB and the maximum ~35 dB. This represents a rather realistic yet challenging wideband front-end example case. The front-end IRR curve is also shown in Fig. 3 (in dash-dot). The total IRR (after compensation) as a function of frequency is obtained by combining (6) and (9), yielding

$$A_{TOT}(f) = \frac{|G_1(f) + W(f)G_2^*(-f)|^2}{|G_2(f) + W(f)G_1^*(-f)|^2} \quad (12)$$

Ordinary raised-cosine pulse-shaping is used with 25 % roll-off and the symbol rates of the two signals are assumed to be 3.84 MHz, yielding roughly a 5 MHz channel bandwidth. Channel spacing is 6 MHz, so after I/Q downconversion the two signals are at ±3 MHz intermediate frequencies. The front-end sampling rate is  $4 \times 3.84 = 15.36$  MHz. The channel is assumed to add only noise (AWGN). The in-band signal-to-noise ratio (SNR) values are in the following given from the desired, weaker, carrier point of view. Three-tap ( $N = 3$ ) compensator is used, and the step-size of the algorithm, with  $P_x$  denoting the power of  $x(t)$ , is  $\text{diag}(1.0 \ 0.5 \ 0.5) \times 10^{-4}/P_x$ . It is selected such, that the convergence time is roughly 1 ms (ca 15000 samples). Power difference between the two carriers is 20 dB.

Fig. 3 shows the ensemble averaged (1000 signal+noise realizations) IRR's before and after compensation with 3-tap and

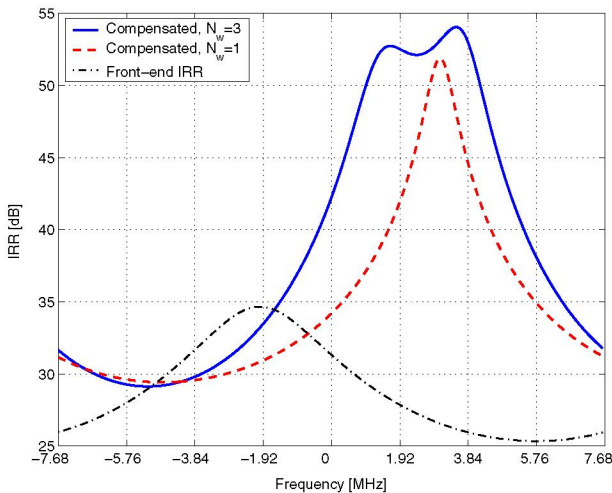


Fig. 3. Example ensemble averaged image-rejection ratios as a function of frequency after compensation with 3-tap (solid) and 1-tap (dashed) compensators. The front-end IRR is in dash-dot. SNR=15 dB and power difference between carriers is 20 dB.

also 1-tap compensators in the steady-state. Clearly, the algorithm approximates the optimum solution better, and hence gives better image rejection in those frequencies where there is strong image interference (or in fact, high image-to-signal power ratio). Thus, in a sense the algorithm is equalizing the signal-to-image power ratio of the processed band. This is of course a very desirable feature. The 1-tap compensator is also performing surprisingly well, with the IRR curve peaking approximately at the center of the interfering signal band. But anyhow, the 3-tap compensator obviously gives better performance, since it takes the frequency-selectivity into account *by design*.

The simulated (uncoded) symbol-error-rate (SER) results in Fig. 4 further verify the excellent performance of the proposed algorithm, the difference between the compensated curve (3-tap) and the AWGN reference being less than 0.5 dB. In the given example scenario, the signal is lost completely without compensation.

## 6. CONCLUSIONS

This paper described an adaptive algorithm for compensating frequency-selective I/Q imbalances in quadrature receivers. The compensation strategy is to make the received signal, which is made improper by the I/Q imbalances, proper again. The proposed algorithm is very general in the sense that it can be used in any quadrature receiver setting, and is independent of any specific structure or characteristic of the ideal received signal other than properness. The algorithm was shown, in a basic two channel low-IF receiver setting, to give high image rejection to the frequency band where there is high image interference, in a sense equalizing the signal-to-image power ratio of the processed band. The SER performance of the algorithm with 16-QAM signals and with a moderate convergence time in the order of 1 ms (or 15000 iterations) was shown to be very good.

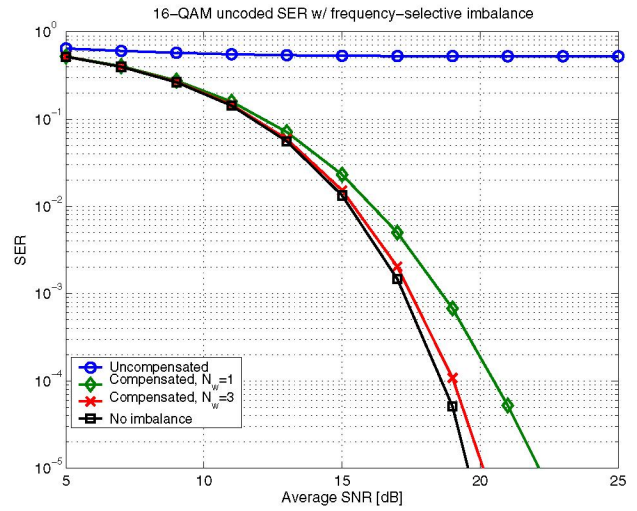


Fig. 4. Uncoded symbol-error-rate for 16-QAM. Shown are the uncompensated, 1-tap compensated, 3-tap compensated, and the AWGN reference. The imbalance parameters are  $g = 3\%$ ,  $\phi = 3^\circ$ ,  $H_I(z) = 0.98 + 0.03z^{-1}$ , and  $H_Q(z) = 1.0 - 0.005z^{-1}$ .

## 7. REFERENCES

- [1] B. Razavi, *RF Microelectronics*. Englewood Cliffs, NJ: Prentice-Hall, 1998.
- [2] S. Mirabbasi and K. Martin, "Classical and modern receiver architectures," *IEEE Commun. Mag.*, vol. 38, pp. 132-139, Nov. 2000.
- [3] M. E. Frerking, *Digital Signal Processing in Communication Systems*. New York: Chapman & Hall, 1994.
- [4] J. Crols and M. S. J. Steyaert, *CMOS Wireless Transceiver Design*. Dordrecht, the Netherlands: Kluwer, 1997.
- [5] M. Valkama, *Advanced I/Q Signal Processing for Wideband Receivers: Models and Algorithms*. Ph.D. Dissertation, Tampere University of Technology, Finland, Dec. 2001.
- [6] A. Tarighat, R. Bagheri, and A. H. Sayed, "Compensation schemes and performance analysis of IQ imbalances in OFDM receivers," *IEEE Trans. Signal Processing*, vol. 53, pp. 3257-3268, Aug. 2005.
- [7] M. Valkama, M. Renfors, and V. Koivunen, "Blind signal estimation in conjugate signal models with application to I/Q imbalance compensation," *IEEE Signal Processing Lett.*, vol. 12, pp. 733-736, Nov. 2005.
- [8] G. Fettweis *et al.*, "Dirty RF," in *Proc. Wireless World Research Forum (WWRF) Meeting 11*, Oslo, Norway, June 2004.
- [9] L. Anttila, M. Valkama, and M. Renfors, "Blind moment estimation techniques for I/Q imbalance compensation in quadrature receivers," in *Proc. 17th Annual IEEE Int. Symp. on Personal, Indoor and Mobile Radio Comm. (PIMRC'06)*, Helsinki, Finland, Sept. 2006.
- [10] J. Tubbax *et al.*, "Compensation of IQ imbalance and phase noise in OFDM systems," *IEEE Trans. Wireless Commun.*, vol. 4, pp. 872-877, May 2005.
- [11] P. J. Schreier and L. L. Scharf, "Second-order analysis of improper complex random vectors and processes," *IEEE Trans. Signal Processing*, vol. 51, pp. 714-725, Mar. 2003.
- [12] B. Picinbono and P. Chevalier, "Widely linear estimation with complex data," *IEEE Trans. Signal Processing*, vol. 43, pp. 2030-2033, Aug. 1995.
- [13] F. D. Neeser and J. L. Massey, "Proper complex random processes with applications to information theory," *IEEE Trans. Information Theory*, vol. 39, pp. 1293-1302, July 1993.
- [14] A. Baier, "Quadrature mixer imbalances in digital TDMA mobile radio receivers," in *Proc. International Zurich Seminar on Digital Communications*, Zurich, Switzerland, March 1990, pp. 147-162.